C. R. Palevol 9 (2010) 369–375

Contents lists available at ScienceDirect

Comptes Rendus Palevol

www.sciencedirect.com

General palaeontology

Bone vascularization and growth in placoderms (Vertebrata): The example of the premedian plate of *Romundina stellina* Ørvig, 1975

Vascularisation et croissance de l'os chez les placodermes (Vertebrata) : l'exemple de la plaque prémédiane de Romundina stellina Ørvig, 1975

Vincent Dupret [a,*], Sophie Sanchez [a,b], Daniel Goujet [c], Paul Tafforeau [b], Per E. Ahlberg [b]

[a] *University of Uppsala, Department of Evolutionary Organismal Biology, Subdepartment of Animal Evolution and Development, Norbyvägen 18A, SE-742 36 Uppsala, Sweden*
[b] *European Synchrotron Radiation Facility, 6, rue Jules-Horowitz, 38043 Grenoble cedex, France*
[c] *Muséum national d'histoire naturelle, département histoire de la Terre, paléontologie, 8, rue Buffon, 75005 Paris, France*

ARTICLE INFO

Article history:
Received 1st March 2010
Accepted after revision 26 July 2010
Available online 28 September 2010

Written on Invitation of the Editorial Board

Keywords:
Bone growth
Phase contrast X-ray synchrotron
Microtomography
Microanatomy
Placodermi
Vascularization

ABSTRACT

The Placodermi (armored jawed fishes), which appeared during the Lower Silurian and disappeared without leading any descendants at the end of the Famennian (Latest Devonian), have the highest diversity of known Devonian vertebrate groups. As phylogenetically basal gnathostomes (jawed vertebrates), they are potentially informative about primitive jawed vertebrate anatomy and origins. Until recently, the study of their internal or histological structures has required destructive methods such as sectioning or serial grinding. Recent advances in tomography and imaging technologies, especially through the increasing use of synchrotron phase contrast imaging for the study of fossils, allow us to reveal the inner structures of the fossil nondestructively and with unprecedented three-dimensional level of detail. Here, we present for the first time the prerostral anatomy of the small acanthothoracid *Romundina stellina*, one of the earliest and most basal placoderms. Phase contrast imaging allows us to reconstruct the vascularization and nerve canals of the premedian plate and adjacent parts of the skeleton three-dimensionally in great detail, providing important clues to the growth modes and biology of the animal.

Mots clés :
Croissance osseuse
Microanatomie
Placodermi
Microtomographie à rayonnement X synchrotron en contraste de phase
Vascularisation

RÉSUMÉ

Les Placodermi (« poissons cuirassés ») apparaissent au Silurien inférieur et disparaissent à la fin du Famennien (Dévonien terminal). Ils présentent la plus grande biodiversité des vertébrés du Dévonien. Ils sont considérés comme les premiers gnathostomes (vertébrés à mâchoires) et, par conséquent, l'étude de leurs fossiles nous apporte des informations cruciales sur l'anatomie des premiers vertébrés à mâchoires et leurs origines. Néanmoins, jusqu'à récemment, l'étude de leur anatomie interne nécessitait des méthodes destructives (sections sériées ou attaques acides). Les avancées récentes dans les domaines de la tomographie et de l'imagerie numérique, et en particulier l'avènement de l'imagerie synchrotron en contraste de phase pour l'étude des fossiles, nous permettent désormais d'accéder à des informations de première importance, sans avoir à endommager des spécimens souvent fort rares de par leurs

* Corresponding author.
E-mail addresses: vincent.dupret@ebc.uu.se (V. Dupret), sophie.sanchez@ebc.uu.se (S. Sanchez), goujet@mnhn.fr (D. Goujet), paul.tafforeau@esrf.fr (P. Tafforeau), Per.Ahlberg@ebc.uu.se (P.E. Ahlberg).

1631-0683/$ – see front matter
doi:10.1016/j.crpv.2010.07.005

préservations exceptionnelles. Nous décrivons ici pour la première fois la neurovascularisation au niveau de la plaque prémédiane (région prérostrale) d'un crâne de petit placoderme acanthothoracide. Cette étude révèle les applications multiples des outils numériques modernes, comme la mise en évidence des relations tridimensionelles des canaux nerveux et vasculaires, de même que l'organisation spatiale de l'os, et permet l'élaboration de modèles de développement biologique pour cet animal.

1. Introduction

The Placodermi (armored fishes) appeared during the Lower Silurian and disappeared without leaving any descendants at the end of the Famennian. They are the most diverse of the known Devonian vertebrate groups (Janvier, 1996). The Placodermi are usually considered the most basal clade of gnathostomes (i.e. jawed vertebrates; Janvier, 1996). Nevertheless, recent studies (e.g. Brazeau, 2009) propose a different phylogenetic background, in which the placoderms are paraphyletic, although still the most basal gnathostomes. Among the Placodermi, the Acanthothoraci (Stensiö, 1944) have been regarded as a polyphyletic or paraphyletic ensemble of primitive placoderms from which the different placoderm clades are derived (Goujet, 1984; Janvier, 1996). Goujet and Young (2004) and Young (2010) viewed them as monophyletic and placed them as the sister group to the Rhenanida at the base of the Placodermi, whereas Brazeau (2009) places the acanthothoracid *Brindabellaspis* immediately above the Antiarchi as the second most basal placoderm taxon. Because of their status as basal placoderms, the Acanthothoraci are potentially highly informative about primitive gnathostome morphology and gnathostome origins.

Until recently, the internal anatomy of early vertebrate fossils could only be investigated by destructive techniques such as mechanical or acid preparation (White, 1952), and serial grinding or sectioning (Poplin and Ricqlès, 1970; Sollas, 1904; Stensiö, 1927, and subsequent works), coupled with three-dimensional (3D) interpretation by wax modelling or graphic techniques that introduced a measure of subjectivity. Fortunately, recent advances in tomography and 3D imaging through the increasing use of phase contrast synchrotron imaging of fossils allow us to perform new nondestructive studies with an unprecedented level of detail (Tafforeau et al., 2006). Here, we present the first results of an investigation of the skull of *Romundina stellina* (Ørvig, 1975) (Fig. 1A), a small acanthothoracid from the Lochkovian (Earliest Devonian) of the Arctic Canadian Archipelago, scanned at the European Synchrotron Radiation Facility (ESRF) in Grenoble, France. The present article describes the snout (prerostral part of the skull) with focus on the premedian plate.

2. Material and methods

2.1. Systematic palaeontology

Class Placodermi McCoy, 1848
Order Acanthothoraci Woodward, 1891
Family Palaeacanthaspididae Stensiö, 1944
Genus *Romundina* Ørvig, 1975
Species *Romundina stellina* Ørvig, 1975
Specimen MNHN CPW 1

Remark concerning the species-level systematic attribution: The specimen studied herein comes from the same locality as the type specimen described by Ørvig (1975; locality 10 in Prince of Wales Island, described in Smith, 1980; figs. 1 and 4). The morphology of the present specimen fits exactly the description provided by Ørvig.

The skull, preserved in three dimensions, was originally enclosed in a limestone matrix. Preparation with 8% formic acid buffered with tricalcium phosphate after mounting the specimen on a resin block has removed the external matrix, but most of the matrix fill inside the skull remains intact.

Anatomical abbreviations: PrM: Premedian plate; pq: attachment area for the palatoquadrate; rc: ethmoidal commissure of the lateral sensory line system.

Institutional abbreviations: CPW: Charles Prince of Wales Island; ESRF: European Synchrotron Radiation Facility; MNHN: Muséum national d'Histoire naturelle, Paris, France.

2.2. Acquisition, treatment and rendering

The sample was scanned on the beam line ID19 of the ESRF with an isotropic voxel size of 7.46 μm with a monochromatic beam set at an energy of 51 keV using a double Si111 crystal monochromator in Bragg reflection. In order to increase the contrast and visibility of fine structures, we used propagation phase contrast effect by setting the distance between the sample and the detector at 900 mm. Phase contrast effect can greatly improve the quality of microtomographic data on fossils in case of insufficient absorption contrast (Tafforeau et al. 2006). We used 1999 projections over 360 degrees with 0.9 seconds of exposure time per projection to benefit of the whole dynamic of the FreLoN CCD camera (Labiche et al., 2007). In order to image the complete specimen, four scans covering 7 mm vertically each were performed. The slices were reconstructed using filtered back projection algorithm (PyHST software, ESRF). The reconstructed slices were then converted into 16 bits tif image stacks that were concatenated to obtain a single stack covering the whole sample. In order to reduce the data size for the general anatomical observations, a second version of the reconstructed scan was calculated with a $2 \times 2 \times 2$ binning and an 8 bits conversion.

Mimics® v.12.3 and v.13.1 (*Materialise*) were used for the 3D modelling (segmentation and 3D object rendering).

VGStudio Max® 2.0 (*Volume Graphics*) was used to model the vascularization.

The internal organization of a bone such as the premedian plate can be made visible by different means using these software packages. In *Mimics*®, there are three options: firstly, by rendering the 3D object transparent (the vacuities in the bone are not selected during segmentation, so in the 3D object all the internal spaces are lined with triangle mesh surfaces which become visible when transparency is applied); secondly, by creating a separate mask in which only the vacuities are filled; and thirdly, by calculating a separate mask with filled internal vacuities from the bone-mask and using a Boolean operation to intersect the two. In *VGStudio Max*®, the vascular mesh can be selected as a "region of interest" thanks to the clear contrast between the vessels and the bone matrix. Because the canals are empty, their connection with the surrounding air has to be cut by using the "opening/closing" tool in order to create a continuous and delimiting surface of the dermal and perichondral bones.

Depending on the desired visualization result, different parallel strategies can be attempted in the selection/segmentation of the structure. For the solid structures we have in this example used two masks, one for the dermal bone (yellow) and one for the perichondral bone (blue; Figs. 1B–D). In some places, the dermal-perichondral boundary has been difficult to pinpoint, but this limitation is more than outweighed by the additional information obtained from separate segmentation of the two ossifications.

3. Results

3.1. The premedian plate

3.1.1. External morphology

The premedian plate (PrM in Fig. 1A, yellow in Figs. 1B–D; median prerostral plate *Prr* of Ørvig, 1975) is an unpaired median dermal element forming the tip of the snout (prerostral ethmoid expansion of the neurocranium), homologous with that of the Antiarchi (Moy-Thomas and Miles, 1971). It is situated anterior to both the orbits and the nasal capsules, which are enclosed in a rostropineal plate forming a rhinocapsular bone unit (not preserved in this specimen), and rests on top of the perichondral bone of the neurocranium (in blue, Figs. 1B–D). The latter is smooth and contiguous with the rest of the cranial perichondral ossification except for the nasal capsule, which was separated by the optic fissure and has been lost in this specimen.

The premedian plate is strongly curved, comprising a raised and strongly convex anterior region and a concave posterior region. The nearly vertical anterior part of the concave region is covered with tiny flat triangular leaf-like tubercles that point dorsally, i.e., away from the nostrils. This suggests that these flat tubercles had a particle filtration role. The rest of the premedian plate is covered in tubercles with indistinctly stellate bases. It is noteworthy that the other plates of the animal display bigger and more obviously stellate tubercles, typical for the Acanthothoraci. The anterior face of the plate shows a deep transverse groove for the ethmoidal commissure of the lateral sensory line system (rc, Fig. 1B); the bottom of this groove exposes a series of minute pores (in green, Figs. 1B1, C1 and D).

The raised convex surface bears a circular structure similar in size to a tubercle, which may represent a silicified encrusting invertebrate exoskeleton (that grew on the plate after the death of the fish) or possibly a parasite cyst (0.3 mm in diameter, visible in Fig. 1B2).

3.1.2. Internal information

In this adult individual (recognizable as such from its well-developed perichondral ossification), the dermal and the perichondral bones (in yellow and blue, respectively, Figs. 1B–D) are very difficult to discriminate where contiguous (Fig. 1C). In other words, the suture between the two types of bone is very faint, and mainly follows the peripheral vascularization of the perichondral bone. This vascularization, which therefore appears at the interface between the perichondral and dermal bone, is in the case of the premedian plate constituted of very big canals, anteroposteriorly oriented and slightly anastomosed (Fig. 2).

The two types of bone also display different thicknesses and organizations depending on which area of the plate is studied. The dermal bone is thinner than the perichondral bone at the posterior end of the plate (Figs. 1C4 and D), whereas in the anterior part (Figs. 1C1–2 and D), the dermal bone is thicker.

The thick anterior half of the premedian plate contains several superimposed levels of vasculature (Figs. 1C2 and 2A1–2). In the thinner areas such as the posterior part of the bone (Figs. 1C3, D and 2A1–2) and along the ethmoidal sensory line commissure (Figs. 1C1, D and 2A1), the dermal bone is less vascularised and there is a greater vascular development in the contact face with the underlying perichondral bone. The posterior margin of the premedian plate is entirely unvascularized; instead the vascular mesh dips down into the perichondral bone where it continues some little distance beyond the edge of the plate.

If the virtual sections indicate that the bone is highly vascularized (in red, Figs. 1C–D and 2), the rendered 3D model plainly reveals the variation in vascular web organization throughout the plate. The posterior half of the plate shows a virtually flat orthogonal vascular web, consisting mainly of anteroposteriorly directed vessels with few transverse canals (anastomoses), the whole being organized as one layer of canals (Figs. 1D and 2). The anterior half shows a completely different organization: the canals form a honeycomb mesh and are organized into four layers (Figs. 1D and 2). The canals of the anterior half seem to converge onto the radiation centre of the plate. It is noteworthy that the most superficial canals, which lie in the semidentine tubercle layer, are much thinner than the underlying ones. The transition between the two patterns occurs in the near-vertical wall that forms the boundary between the posterior concave and anterior convex regions, where the thickness of the bone increases anterior ward (Figs. 1D and 2). The presence of these two different patterns in one bone has not been found in any other part of the dermal skull roof than the premedian plate.

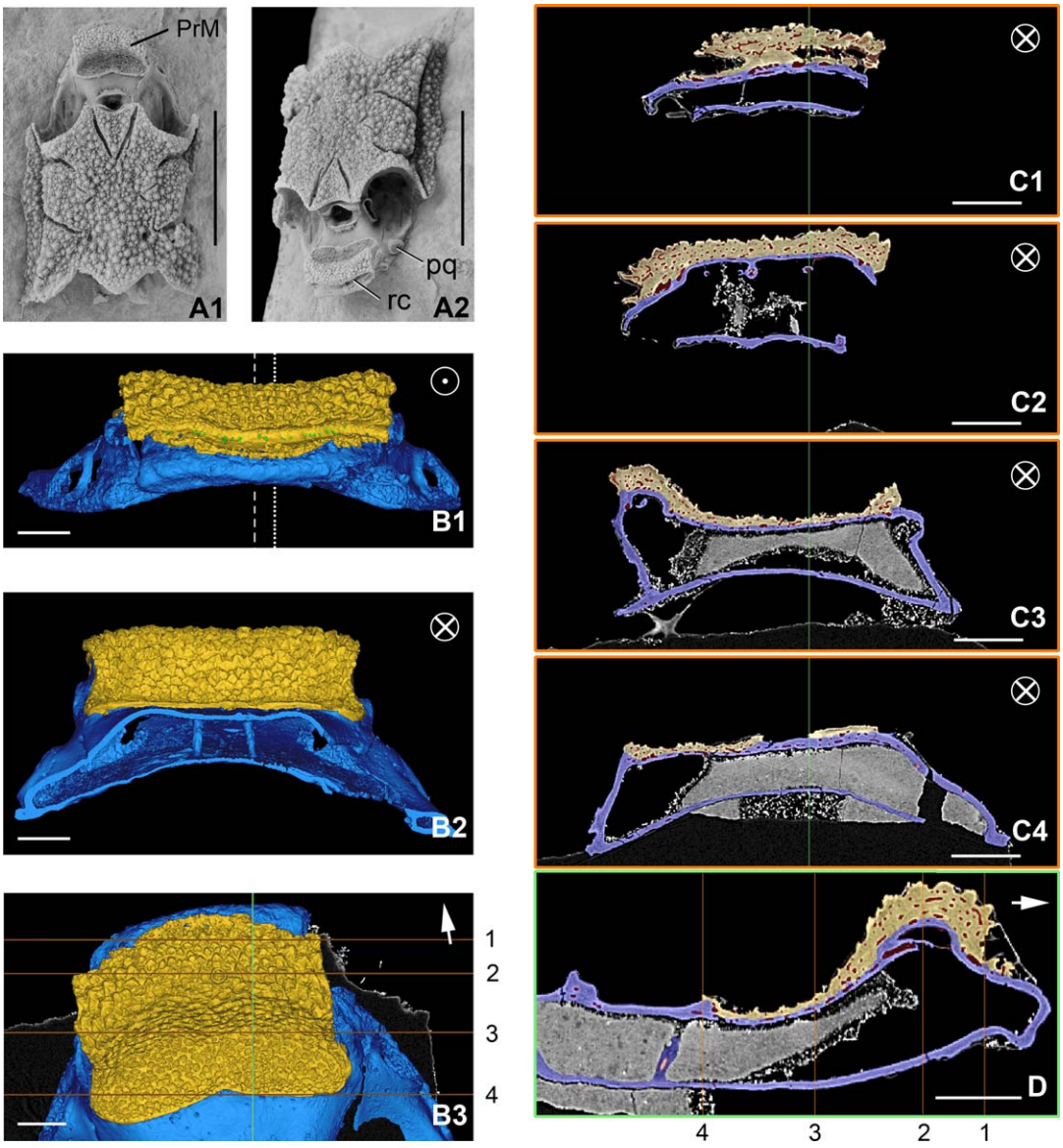

Fig. 1. *Romundina stellina* Ørvig, 1975, specimen MNHN CPW 1. **A**. Skull in dorsal (A1) and oblique anterodorsal (A2) views. **B**. Reconstruction of the premedian plate and of the ethmoid part of the neurocranium in anterior (B1), posterior (B2) and dorsal (B3) views. **C**. Virtual transverse sections along the premedian plate and the ethmoid part of the neurocranium, at the level of the ethmoidal commissure (C1), at the topmost part of the plate (C2), along the level of the vertical wall of the plate (C3), and at the posterior edge of the plate (C4). **D**. Virtual paralongitudinal section along the premedian plate and the ethmoid part of the neurocranium. Dashed line on B1 corresponds to the midline of the premedian plate; notice that the symmetry plane for the sensory line pores (dotted line) is slightly shifted to the left of the animal. Orange lines labelled from 1 to 4 in B3 and D correspond to the position of the virtual sections shown in C1–4; green line in B3 and C1–3 corresponds to the position of virtual section shown in D. On both virtual sections and reconstructions, the dermal bony premedian plate appears in yellow, the "perichondral" bone in blue, the vascularization in red (C, D), and the ethmoidal commissure of the sensory line system in green (B1, C1). Matrix and glue appear in grey. **PrM**, premedian plate; **pq**, attachment area for the palatoquadrate; **rc**, ethmoidal commissure of the sensory line system. Arrows indicate foreward. Scale bars for A: 1 cm; scale bars for B–D: 1 mm. Three dimensional models made with *Mimics*® v. 12.3 (*Materialise*).

Fig. 1. *Romundina stellina* Ørvig, 1975, spécimen MNHN CPW 1. **A**. Crâne en vues dorsale (A1) et antérodorsale oblique (A_2). **B**. Reconstitution de la plaque prémédiane et de la partie antérieure de l'os périchondral en vues antérieure (B1), postérieure (B2) et dorsale (B3). **C**. Coupes transversales virtuelles en différents endroits de la plaque prémédiane : au niveau de la commissure ethmoïdienne (C1), au sommet de la plaque (C2), au niveau du mur vertical (C3), et dans le bord postérieur de la plaque (C4). **D**. Coupe paralongitudinale virtuelle le long de la partie prérostrale du crâne. La ligne en tiretés correspond au plan de symétrie de la plaque; remarquer que le plan de symétrie de la commissure ethmoïdienne (en pointillés) est légèrement déjeté vers la gauche de l'animal. Les lignes orange numérotées de 1 a 4 en B3 et D correspondent aux coupes virtuelles transversales montrées en C1–4; la ligne verte en B_3 et C1–3 correspond à la coupe virtuelle paralongitudinale montrée en D. Dans les coupes virtuelles et les modèles tri-dimensionnels (3D), l'os dermique de la plaque prémédiane apparaît en jaune, l'os périchondral en bleu, la vascularisation en rouge (C–D), et la partie identifiée du système de la commissure ethmoïdienne en vert (B1, C1). La matrice et la colle apparaissent en niveaux de gris. **PrM**, plaque prémédiane ; **pq**, surface d'insertion du palatocarré ; **rc**, sillon de la commissure ethmoïdienne. Les flèches indiquent l'avant. Barres d'échelle pour A : 1 cm ; pour B–D : 1 mm. Modèles 3D générés sous *Mimics*® v. 12.3 (*Materialise*).

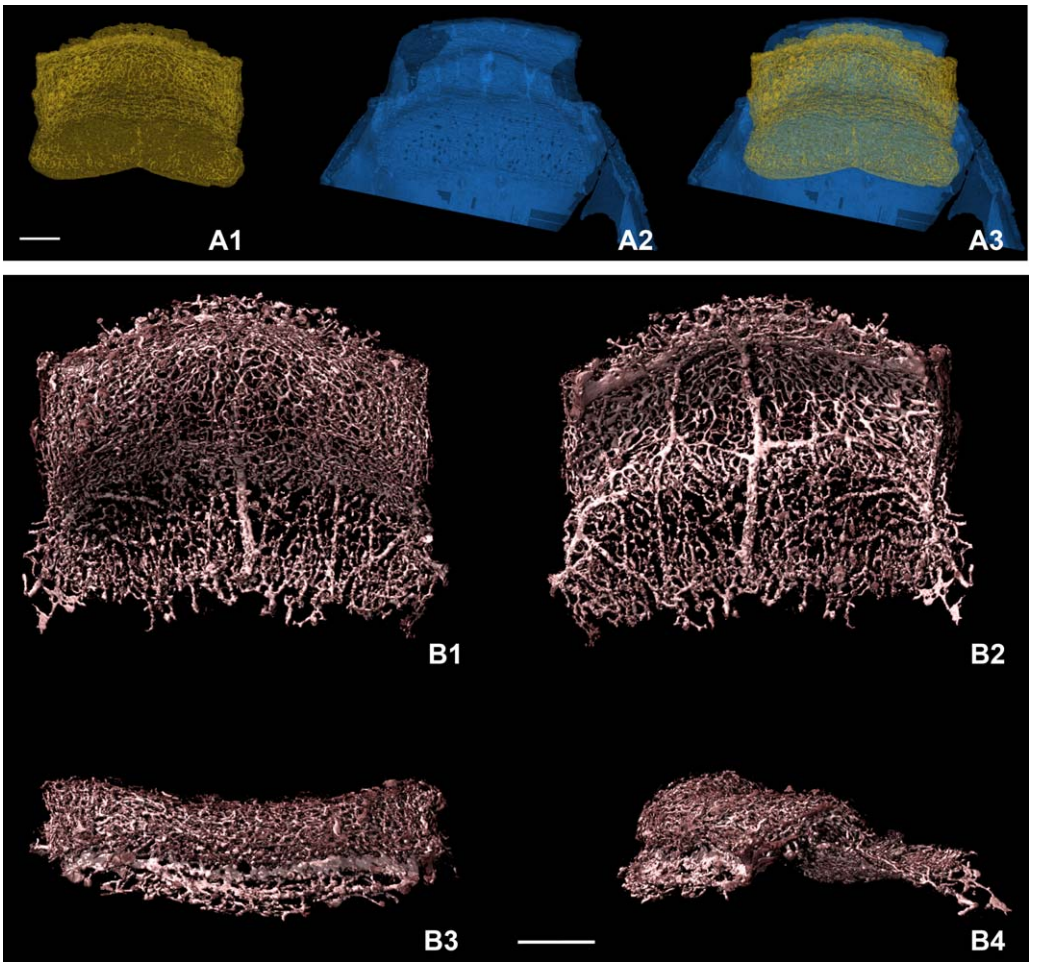

Fig. 2. *Romundina stellina* Ørvig, 1975, specimen MNHN CPW 1. Prerostral region of the skull. **A.** Premedian plate (A1), underlying perichondral bone (A2), and both dermal structures (A3) in dorsal views, seen by transparency and showing the neurovascular web. **B.** Neurovascularization of the premedian plate and the underlying perichondral bone, in dorsal (B1), ventral (B2), anterior (B3) and oblique left anterolateral (B4) views. Scale bars: 1 mm.
A was made using *Mimics*® (*Materialise*) v. 12.3; **B** was made using *VGStudio Max* v. 2.0 (*Volume Graphics*).
Fig. 2. *Romundina stellina* Ørvig, 1975, spécimen MNHN CPW 1. Région prérostrale du crâne. **A.** Plaque prémédiane (A1), os périchondral sous-jacent (A2), et de l'ensemble (A3) en vues dorsales, transparentes et montrant le réseau de canaux neurovasculaires. **B.** Neurovascularisation de la plaque prémédiane et de l'os périchondral sous-jacent, en vues dorsale (B1), ventrale (B2), antérieure (B3) et oblique antérolatérale gauche (B_4). Barres d'échelle : 1 mm.

The whole vascular mesh is traversed by a large, median, anteroposteriorly directed canal. Posteriorly, this canal runs along the contact between perichondral and dermal bone, but anteriorly where the endoskeleton rises into a "shoulder" that supports the convex region of the premedian plate it dips below the perichondral shell and tunnels through the cartilaginous core of the endoskeleton, surrounded by its own perichondral tube. Anteriorly, it is connected to a large, flattened, transverse canal web located just internal to the bottom of the ethmoid commissure sensory line groove, between the perichondral and dermal ossifications. The large median canal is surrounded by a pair of lateral parallel smaller ones, which follow similar trajectories, and connected to them by a pair of oblique canals (Figs. 2B1–2; note that the arrangement of the bigger canals is slightly different in the material described by Ørvig, 1975: pl. 1 fig. 4; pl.3 fig. 5). The transverse web is a paired structure, with left and right halves meeting near the midline, but in an asymmetric, and unorganized way (Fig. 3A). It extends laterally to leave the premedian plate (most likely to continue on the suborbital plate; see Ørvig, 1975: figs. 1A and 2A). Short canaliculi (in green, Figs. 1C1, D and 3) that probably transmitted the nerve fibres to the neuromast organs of the ethmoidal sensory line commissure extend from the transverse web into the bottom of the groove that housed the sensory line. (Fig. 1B1). The web thus housed both nerves and blood vessels. The openings of the canaliculi are aligned along the ethmoidal commissure with a precise symmetrical pattern, though shifted slightly to the left regarding the geometric midline of the plate itself (Figs. 3A–B; we are uncertain whether this is either the norm or an individual variation). It is noteworthy that the transverse web is flattened, whereas the rest of the vascularization is obviously cylindrical in section (Figs. 2B2–4 and 3A); this is probably a function of its large size combined with its location in the

contact surface between dermal and endoskeletal ossifications (Fig. 3).

3.2. Endoskeleton

The scan reveals a characteristically placoderm architecture for the endoskeleton, with a well-developed perichondral bone envelope but no trace of endochondral ossification. Neither is there any sign of calcified cartilage. The articular surfaces for the palatoquadrate, which are located anteriorly on the suborbital-ethmoidal shelf close to the premedian plate (pq, Figs. 1A2 and B1), form holes in the perichondral envelope. Several pores corresponding to vessel exits are visible on the ventral side of the dorsal wall of the perichondral bone (below the thin posterior half of the premedian plate; see also Ørvig, 1975: pl. 1 fig. 4; pl.3, fig. 5). An unexpected discovery is a pair of anterodosally directed "pillars" running between the floor and roof of the prerostral region of the ethmoid area (Fig. 1B2): each transmits a narrow canal that we interpret as a nerve canal. We tentatively infer that they may have transmitted branches of the palatine nerve that supplied tactile sense organs in the area around the nostrils.

4. Discussion

The distinct geometries of the different vascular components in the premedian plate and on the surface of the perichondral bone provide clues to the growth processes that shaped this region. The manner in which the large anteroposteriorly oriented canals cut through the endoskeletal "shoulder" before reaching the anterior transverse neurovascular web (Fig. 2B1–2) is central to the interpretation. Given that each vessel is wrapped in perichondral bone, and thus in life was wrapped in periosteal (originally perichondral) membrane, it strongly suggests that the vessels were in place before the "shoulder" developed by differential growth of the cartilage; in other words, the cartilage grew up between and engulfed the vessels. The premedian plate is a rigid structure composed of dermal bone, and notwithstanding the possibility of remodelling through resorption (Donoghue et al., 2006) it seems likely that it did not reach its full dimensions until the underlying cartilage had achieved more or less its adult shape (although not its adult size). We can therefore conclude that the major anteroposterior vessels and transverse neurovascular web were established before the premedian plate achieved its adult concavo-convex shape, and possibly before it started mineralizing at all.

Together, these vessels evidently irrigated and drained the "upper lip" area including the ethmoidal sensory line commissure, but the direction of the blood flow cannot be determined with certainty. However, the nerve supply for the sensory line commissure was, by comparison with living vertebrates such as *Amia* (Jarvik, 1980), probably supplied by the left and right rami of the buccalis lateralis of the trigeminal nerve, entering at the lateral ends of the transverse neurovascular web.

The radially organized honeycomb vascular mesh of the thick anterior part of the premedian plates centers on a point close to where the large midline vessel meets the

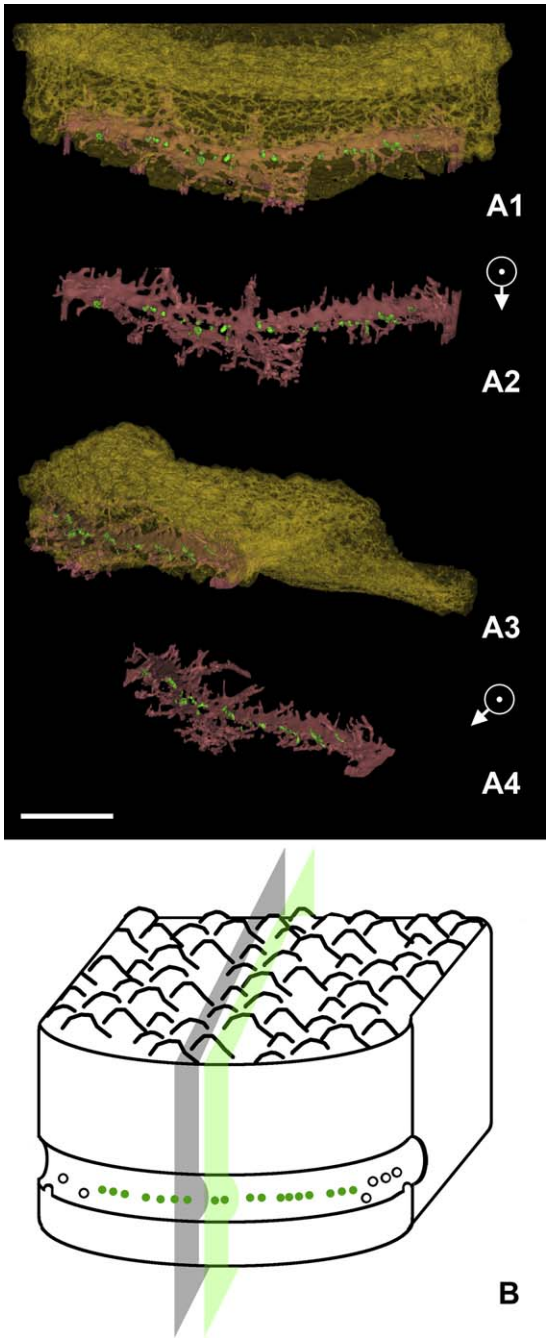

Fig. 3. *Romundina stellina* Ørvig, 1975, specimen MNHN CPW 1. **A.** Premedian plate and its neurovascularization in anterodorsal view (A1–2) and in oblique left lateral view (A3–4). Premedian plate is transparent yellow, vascularization is red, sensory canalicles of the ethmoidal commissure in green. **B.** Schematic reconstruction of the premedian plate illustrating the shift between the symmetry plane of the plate (in grey) and that of the ethmoidal commissure (in green). Scale bars in **A**: 1 mm; **B**: not at scale.

Fig. 3. *Romundina stellina* Ørvig, 1975, spécimen MNHN CPW 1. **A.** Plaque prémédiane et sa neurovascularisation en vues antérodorsale (A1–2) et oblique latérale gauche (A3–4). La plaque prémédiane apparaît en jaune transparent, la vascularisation en rouge et les canalicules de la commissure ethmoïdienne en vert. **B.** Reconstitution schématique de la plaque prémédiane montrant la non-superposition des plans de symétrie de la plaque (en gris) et de la commissure ethmoïdienne (en vert). Barre d'échelle de **A** : 1 mm ; **B** : non à l'échelle.

transverse web. This is evidently the growth centre of the dermal ossification, which has expanded posteriorly and laterally from here to cover the whole convex "shoulder" of the endoskeleton. However, in the thinner posterior part of the plate, the vascularization shows no such radial pattern, and as already noted the vessels descend into the perichondral bone just before the posterior plate margin. There is a quite sharp transition between the radial and nonradial patterns, at the point where the large vessels pierce the "shoulder" of the endoskeleton (Fig. 1B2 and animation). It seems probable that the posterior nonradial vascular mesh developed in the contact surface between the endoskeleton and the overlying incipient ossification of the premedian plate, and could then become incorporated into either the dermal or the perichondral bone.

The very elaborate internal vascularization of the premedian plate implies an enormous surface area of vascular-bone contact within the plate. This was probably linked to the role of the bone as a site of phosphate deposition and extraction (correlated to the production Adenosine TriPhosphate [ATP]) though it may well have had additional functions. At any rate, it is interesting to note that no such vascularization is present in the perichondral bone except in the contact area with the posterior part of the premedian plate.

The observation by one of us (D. G.) of an isolated premedian plate of a juvenile individual of *R. stellina* reveals that the basal lamellar layer is lacking at this ontogenetic stage. Evidently, this plate was not yet "fused" (i.e., connected) to underlying perichondral bone, and it is quite likely that the perichondral bone layer of the neurocranium was not yet formed. This means that the premedian plate only became firmly attached to the underlying neurocranium at a relatively late stage in ontogeny.

5. Conclusion and perspectives

The recent advances in synchrotron imaging technologies allow us to uncover very fine structures in 3D, without involving the destruction of the studied specimen. The present study of the premedian plate of an adult specimen of *Romundina* reveals a complex vascular organization. The differences observed between the widely spread vascularization of the dermal plate and the more orthogonal and only slightly anastomosed condition observed in the perichondral bone (and the posterior half of the plate) allow us to draw some preliminary conclusions about the process of bone formation and connection between the dermal and perichondral bone.

Further studies involving the rest of the skull roof, as well as other taxa, will undoubtedly increase our knowledge of the biology of these fishes and, more generally, of the deepest vertebrate and gnathostome representatives of our evolutionary tree.

Acknowledgements

The specimen of *R. stellina* was collected by Daniel Goujet during an expedition in the Arctic Canadian Archipelago in 1995. The photographs were taken by Philippe Loubry (CNRS-MNHN). We gratefully acknowledge the support of ESRF (project EC-203). Ahlberg, Dupret and Sanchez are supported by ERC Advanced Investigator grant 233111. Ahlberg also acknowledges the support of Vetenskapsrådet (the Swedish Research Council). We also thank the two anonymous reviewers for their interest and very constructive comments.

Appendix A. Supplementary online information

Supplementary data associated with this article can be found, in the online version, at doi:10.1016/j.crpv.2010.07.005.

References

Brazeau, M.D., 2009. The braincase and jaws of a Devonian 'acanthodian' and modern gnathostome origins. Nature 457, 305–308.
Donoghue, P.C.J., Sansom, I.J., Downs, J.P., 2006. Early evolution of vertebrate skeletal tissues and cellular interactions, and the canalization of skeletal development. J. Exp. Zool. (Mol. Dev. Evol.) 306B, 278–294.
Goujet, D., 1984. Placoderm Interrelationships: a new Interpretation, with a short review of Placoderm Classifications. Proc. Linnean Soc. N. S. W. 107, 211–243.
Goujet, D., Young, G.C., 2004. Placoderm anatomy and phylogeny: new insights. In: Arratia, G., Wilson, M.V.H., Cloutier, R. (Eds.), Recent Advances in the Origin and Early Radiation of Vertebrates. Verlag Dr. Friedlich Pfeil, München, Germany, pp. 109–26.
Janvier, P., 1996. Early Vertebrates. Oxford Science Publications, Oxford.
Jarvik, E., 1980. Basic structure and evolution of the vertebrates. Academic Press, London and New York.
Labiche, J.C., Mathon, O., Pascarelli, S., Newton, M.A., Ferre, G.G., Curfs, C., Vaughan, G., Homs, A., 2007. The fast readout low noise camera as a versatile X-ray detector for time resolved dispersive extended X-ray absorption fine structure and diffraction studies of dynamic problems in materials science, chemistry, and catalysis. Rev. Sci. Instrum., 78-091301.
McCoy, F., 1848. On some new fossil fish of the Carboniferous period. Ann. Mag. Nat. Hist. 2, 1–10.
Moy-Thomas, J.A., Miles, R.S., 1971. Paleozoic fishes, Second edition. Chapman & Hall, London.
Ørvig, T., 1975. Description, with special reference to the dermal skeleton, of a new Radotinid arthrodire from the Gedinnian of Arctic Canada, Extrait des Colloques internationaux du Centre National de la Recherche Scientifique. Probl. Actuels Paleontol. Evol. Vertébrés 218, 41–71.
Poplin, C., Ricqlès, A.D., 1970. A technique of serial sectionning for the study of the undecalcified fossils. Curator 13, 7–20.
Smith, R.E., 1980. Lower Devonian (Lochkovian) biostratigraphy and brachiopod faunas, Canadian Arctic Islands. Bull. Geol. Surv. Can. 308, 1–155.
Sollas, W.J., 1904. A method for the investigation of fossils by serial sections. Trans. Royal Soc. Lond. B196, 259–265.
Stensiö, E., 1927. The Downtonian and Devonian vertebrates of Spitsbergen. I. Family Cephalaspidae. Skrifter om Svalbard og Ishavet 12, 1–391.
Stensiö, E., 1944. Contributions to the knowledge of the vertebrate fauna of the Silurian and Devonian of Podolia II – Note on two Arthrodires from the Downtonian of Podolia. Arkiv för Zoologi 35, 1–83.
Tafforeau, P., Boistel, R., Boller, E., Bravin, A., Brunet, M., Chaimanee, Y., Cloetens, P., Feist, M., Hoszowska, J., Jaeger, J.J., Kay, R.F., Lazzari, V., Marivaux, L., Nel, A., Nemoz, C., Thibault, X., Vignaud, P., Zabler, S., 2006. Applications of X-ray synchrotron microtomography for nondestructive 3D studies of paleontological specimens. Appl. Phys. A Materials Sci. Processing 83, 195–202.
White, E.I., 1952. Australian Arthrodires. Bull. Br. Natl. Hist. (Geol.) 1, 249–304.
Woodward, A.S., 1891. Catalogue of the fossil fishes in the British Museum of Natural History. Part II. Containing the Elasmobranchii (Acanthodii), Holocephali, Ichthyodorulites, Ostracodermi, Dipnoi, and Teleostomi (Crossopterygii) and chondrostean Actinopterygii. Br. Museum Nat. Hist. (Lond.).
Young, G.C., 2010. Placoderms (armored fish): dominant vertebrates of the Devonian period. Annu. Rev. Earth Planet. Sci. 38, 523–550.